J. Neurogenetics, 28(3–4): 374–388

ISSN: 0167-7063 print/1563-5260 online
DOI: 10.3109/01677063.2014.891590

informa
healthcare

Original Research Article

Multiple Redundant Medulla Projection Neurons Mediate Color Vision in *Drosophila*

Krishna V. Melnattur[1], Randall Pursley[2], Tzu-Yang Lin[1], Chun-Yuan Ting[1], Paul D. Smith[3], Thomas Pohida[2] and Chi-Hon Lee[1]

[1]Section on Neuronal Connectivity, Laboratory of Gene Regulation and Development, *Eunice Kennedy Shriver* National Institute of Child Health and Human Development, National Institutes of Health, Bethesda, Maryland, USA
[2]Signal Processing and Instrumentation Section, Division of Computational Bioscience, Center for Information Technology, National Institutes of Health, Bethesda, Maryland, USA
[3]Laboratory of Cellular Imaging and Macromolecular Biophysics, National Institute of Biomedical Imaging and Bioengineering, National Institutes of Health, Bethesda, Maryland, USA

Abstract: The receptor mechanism for color vision has been extensively studied. In contrast, the circuit(s) that transform(s) photoreceptor signals into color percepts to guide behavior remain(s) poorly characterized. Using intersectional genetics to inactivate identified subsets of neurons, we have uncovered the first-order interneurons that are functionally required for hue discrimination in *Drosophila*. We developed a novel aversive operant conditioning assay for intensity-independent color discrimination (true color vision) in *Drosophila*. Single flying flies are magnetically tethered in an arena surrounded by blue and green LEDs (light-emitting diodes). The flies' optomotor response is used to determine the blue-green isoluminant intensity. Flies are then conditioned to discriminate between equiluminant blue or green stimuli. Wild-type flies are successfully trained in this paradigm when conditioned to avoid either blue or green. Functional color entrainment requires the function of the narrow-spectrum photoreceptors R8 and/or R7, and is within a limited range, intensity independent, suggesting that it is mediated by a color vision system. The medulla projection neurons, Tm5a/b/c and Tm20, receive direct inputs from R7 or R8 photoreceptors and indirect input from the broad-spectrum photoreceptors R1–R6 via the lamina neuron L3. Genetically inactivating these four classes of medulla projection neurons abolished color learning. However, inactivation of subsets of these neurons is insufficient to block color learning, suggesting that true color vision is mediated by multiple redundant pathways. We hypothesize that flies represent color along multiple axes at the first synapse in the fly visual system. The apparent redundancy in learned color discrimination sharply contrasts with innate ultraviolet (UV) spectral preference, which is dominated by a single pathway from the amacrine neuron Dm8 to the Tm5c projection neurons.

Keywords: color discrimination, medulla projection neurons, neural substrate, visual behavior

INTRODUCTION

Color vision, the ability to differentiate spectral properties independent of light intensity, affords object recognition and pattern discrimination, and has been demonstrated in many visual animals, from primates to insects (Jacobs, 2009; Goyret et al., 2008; Menzel & Greggers, 1985). Color percepts in the brain are thought to result from the action of sequential processes that transform a photoreceptor activation pattern in the eye into a hue-based representation in higher brain centers (reviewed in Stockman & Brainard, 2010). The identities, spectral sensitivities, and retinal distribution of the photoreceptors that mediate the first stage of color vision are well characterized (Nathans, 1999). Substantial progress has been made in identifying retinal circuits that combine photoreceptor outputs into segregated chromatically opponent ganglion cell pathways (reviewed in Dacey, 2004; Field & Chichilnisky, 2007). These cells have response characteristics that suggest they might be the neural implementation of the second stage of color processing. However, the functional relationship of these opponent ganglion cell pathways to behavioral hue discrimination remains unclear. Indeed, the electrophysiologically defined opponent axes

Received 17 December 2013; accepted 3 February 2014.
Address correspondence to Chi-Hon Lee, MD, PhD, Section on Neuronal Connectivity, Laboratory of Gene Regulation and Development, *Eunice Kennedy Shriver* National Institute of Child Health and Human Development, National Institutes of Health Building 18T, Room 106, MSC 5431, Bethesda, MD 20892, USA. E-mail: leechih@mail.nih.gov

do not precisely match the perceptually defined opponent axes (discussed in Neitz & Neitz, 2011). Furthermore, there are hypothesized to be up to 8 perceptually defined opponent axes, far greater than the number of physiologically defined opponent axes observed in the primate retina (Webster & Mollon, 1991). Finally, despite recent progress in determining retinal connectomes (Helmstaedter et al., 2013), the daunting complexity of the primate nervous system, and limited range of genetic tools, means that establishing a causal deterministic relationship between a morphologically or electrophysiologically defined class of neurons and functional visual discrimination remains very challenging.

Drosophila, with its compact nervous system, wide range of visual behaviors, and a plethora of sophisticated genetic tools for manipulation of circuit function is excellently positioned to fill this gap between circuit and behavior (reviewed in Borst, 2009; Meinertzhagen & Lee, 2012). The fly visual system is composed of the compound eye and four optic neuropils—the lamina, medulla, lobula, and lobula plate. Each ommatidium of the fly compound eye has eight photoreceptors, divided into three classes based on their relative position and opsin expression. The "outer" photoreceptors R1–R6, which express the opsin Rh1, respond to a broad spectrum of light and mediate motion detection (O'Tousa et al., 1985; Heisenberg & Buchner, 1977). The inner photoreceptors R7 and R8 express opsins that respond to a more restricted range of wavelengths in a complex pattern (Hardie, 1979; Mikeladze-Dvali et al., 2005), mediate chromatic discrimination (Gao et al., 2008; Schnaitmann et al., 2010; this study), and are thus presumed to be analogous to vertebrate cone cells. In the "pale" type ommatidia, R7 cells express the Rh3 opsin, which is maximally sensitive to ultraviolet (UV), and R8 cells express the Rh5 opsin, which is maximally responsive to blue. In the "yellow" ommatidia, R7s express the Rh4 opsin, maximally sensitive to long UV and the underlying R8s express the Rh6 opsin, maximally sensitive to green. The pale and yellow ommatidia are randomly distributed in the retina in a 30:70 ratio, and presumably extend the spectral range of the retina to mediate color vision (Morante & Desplan, 2008).

All visual information received by photoreceptors converges on the medulla: R8 and R7 photoreceptors project axons directly to two distinct layers in the medulla, whereas lamina neurons L1–L3 relay information from R1–R6 to various medulla layers (Fischbach & Dittrich, 1989). The medulla neuropil is composed of $>50{,}000$ neurons organized into ~60 morphologically defined classes in layers and retinotopic columns (Fischbach & Dittrich, 1989). Recent studies have made significant progress towards determining the medulla neurons that receive R7 and R8 inputs (Gao et al., 2008, Karuppudurai et al., 2014; Takemura et al., 2013). These include amacrine neurons that are intrinsic to the medulla as well as projection neurons that connect the medulla to the lobula. In particular, the medulla projection neurons Tm5a/b/c, Tm9, and Tm20 receive direct input from R8 and R7 photoreceptors as well as indirect retinotopic input from R1–R6 photoreceptors via the lamina neuron L3, and indirect pooled R7 input from the amacrine neuron Dm8, and relay chromatic information to deeper regions of the optic lobe, suggesting that they are anatomically analogous to vertebrate retinal ganglion cells (Cajal & Sanchez, 1915; Sanes & Zipursky, 2010). Thus, *Drosophila*, appear to have the "hardware" necessary to implement a color vision system. Furthermore, intensity-independent hue discrimination (so-called "true" color vision) has been demonstrated in bees, butterflies, and hawkmoths (Crane, 1955; Kelber, 1996; Srinivasan, 2010): bees have three kinds of spectral photoreceptors and are trichromats, like humans and New World primates (Srinivasan, 2010), whereas butterflies possess up to eight kinds of spectral photoreceptors and have been shown to be functional tetrachromats, capable of wavelength discrimination in the 1 nm range (Koshitaka et al., 2008). Insects thus display very sophisticated color discrimination abilities. However, despite a long history of probing visual behaviors, the specific medulla circuits that mediate color vision in flies remain unknown.

Here, we report the development of a novel aversive operant conditioning paradigm for true color vision in flies. Using the color-blind optomotor response, we determined the point of blue-green isoluminance for wild-type flies, and were able to condition flies to discriminate between equiluminant blue and green lights. We show that this learned discrimination ability requires the function of the narrow-spectrum photoreceptors R8 and/or R7, and is intensity independent within a limited range, both requirements of an assay for true color vision. Finally, we demonstrate that four classes of medulla projection neurons redundantly mediate functional hue discrimination in our assay. This work represents the first demonstration of the requirement of specific classes of medulla neurons for functional hue discrimination and further suggests that the fly represents color along multiple axes after the first synapse in the visual system.

METHODS

Fly Strains

Fly stocks were maintained on standard fruit fly medium at 25°C under 12/12-hour dark/light cycle. Flies for behavior experiments were reared in medium supplemented with β-carotene (0.295g/L). Fly stocks used in this study are listed below:

(1) *norpA*^{36}; *Rh1-norpA* (a gift from Craig Montell)
(2) *ort*^{C1a}*-Gal4* (labels Tm5a/b/c and Tm20, Karuppudurai et al., 2014)

(3) *ort^{C1a}-LexA::VP16* (designated *ort^{C1a}-LexA*)
(4) *ort^{C1a}-DBD*
(5) *ort^{C1a}-LexADBD*
(6) +; *ort^{C1a}-DBD* ; *ET24g-dVP16AD* (designated *Tm5ab-GAL4*, labels Tm5a/b)
(7) +; *ort^{C1a}-DBD, OK371-dVP16AD* (designated *Tm5c-GAL4*, labels Tm5c)
(8) +; *ort^{C1a}-DBD*, *ET9A-dVP16AD* (designated *Tm20-GAL4*, labels Tm20)
(9) +; *ort^{C1a}-DBD, OK371-dVP16AD*/+; *ET24g-dVP16AD* (designated *Tm5abc-GAL4*, labels Tm5a/b, Tm5c)
(10) *ort^{C1a}-lexADBD*/+; *ET24a-dVP16AD* (designated *Tm20-LexA*, labels Tm20)
(11) +; *ort^{C1a}-DBD*, *ET9A-dVP16AD / OK371-dVP16AD* (designated *Tm5c + 20-GAL4*, labels Tm5c and Tm20)
(12) +; *ort^{C1a}-DBD*, *ET9A-dVP16AD*; *ET24g -dVP16AD* (designated *Tm5ab + 20-GAL4*, labels Tm5a/b and Tm20)
(13) *UAS > CD2,y+ > mCD8::GFP* (for single-cell flip-out experiments)
(14) *UAS-mCD8::GFP*
(15) *UAS-TNT-E* (Sweeney et al., 1995)
(16) *13XLexAop2-IVS-TNT::HA* (designated *LexAop-TNT::HA*)
(17) *hsFLP^{122}*

Color Flight Arena

Color visual stimuli, corresponding rotational tracking response measurements, and heat aversive stimuli were conducted with an automated system. The instrumentation consisted of (1) a flight arena for holding single tethered flies and presenting visual stimuli, (2) a video camera for video acquisition, (3) a near-infrared laser for administrating aversive stimuli, and (4) a PC computer running custom LabVIEW program (National Instruments, Austin, TX) for logging experimental data and integrated hardware control (Figure 1a and b).

The fly, with attached steel pin, was held in the magnetic field between two sets of vertically aligned rare earth magnets (Magcraft, Vienna, VA), a rod magnet on top and a stack of ring magnets at the bottom (Figure 1b) as previously described (Duistermars & Frye, 2008; Bender & Dickinson, 2006). The flight arena consisted of the magnets and an octagonal arrangement of eight 8×8 tricolor light-emitting diode (LED) arrays (Sparkfun, Boulder, CO). The wavelengths of the blue and green LEDs, measured using a spectroradiometer (PR-670; Photo Research, Chatsworth, CA), are 470 and 528 nm, respectively. The light intensity (in $\mu W/cm^2$) was measured using a photodiode power sensor (S120UV; Thorlabs, Newton, New Jersey, USA) and optical power meter (PM300E; Thorlabs) in the calibrated range (200–1100 nm). The interior of the arena had a diameter of 14.4 cm and a height of 7.2 cm. Each LED subtended approximately 5.6° in the horizontal plane. Each LED array was controlled by a custom control board utilizing the PAK-Vc chip (AWC Electronics, League City, TX), which uses pulse-width modulation (at 1.9 kHz) to provide 8-bit intensity resolution (0–255) for each column of the LED array. In the open-loop configuration, predetermined sequences of light patterns were generated by the controlling LabVIEW program. Variables included the number of trials, the color the subject should track, the duration of each trial, and the rest time between trials. The commands required for refreshing the patterns were sent to the LED control boards via two serial ports at run time.

The video monitoring was accomplished with a near-infrared-sensitive video camera (LTC0385/20; Bosch Security, Stuttgart, Germany) positioned for a bottom view and digitized with a frame-grabber card (PCI-1409; National Instruments). A circular array of infrared LEDs (940 nm), positioned around the ring magnets below the tethered fly, was used to illuminate the tethered flies. A long-pass filter, placed in front of the camera, was used to remove interfering light from visual stimuli and near-IR laser. The video images were acquired with a resolution of 480×480 at 10 frames/second, displayed on the graphical user interface (GUI), and saved into an AVI movie format. The images were processed in real time with a correlation-based pattern-matching algorithm provided by the LabVIEW Vision Development Module. The orientation of the subject was calculated by the pattern-matching algorithm by correlating the experimental images to a stored reference image of the subject acquired before the start of the experiment. The reference image was adjusted so the subject's orientation was at zero degrees.

A near-infrared (NIR) laser (810 nm; OPC-A001-FC/60; OptoPower, Tucson, AZ) was triggered using a data acquisition module (USB-6211; National Instruments) to provide negative reinforcement to the flies when the subjects strayed from the target color. After recording of initial configuration for an experiment, data were recorded on a frame-by-frame basis. For each frame, the current time and date, the state of the stimuli, the state of the NIR laser, and the orientation of the training subject were recorded in a log file for future analysis.

Training Paradigm

Flies were tethered to 0.1 mm diameter stainless minutien pins (Fine Science Tools, Foster City, CA) with UV-activated glue under cold anesthesia using procedures previously described (Bender & Dickinson, 2006; Duistermars & Frye, 2008). Three- to five-day-old female flies were used for tethering; the pins were trimmed to a length of 7 mm. Tethered flies were allowed to recover from anesthesia for 1–3 hours before testing.

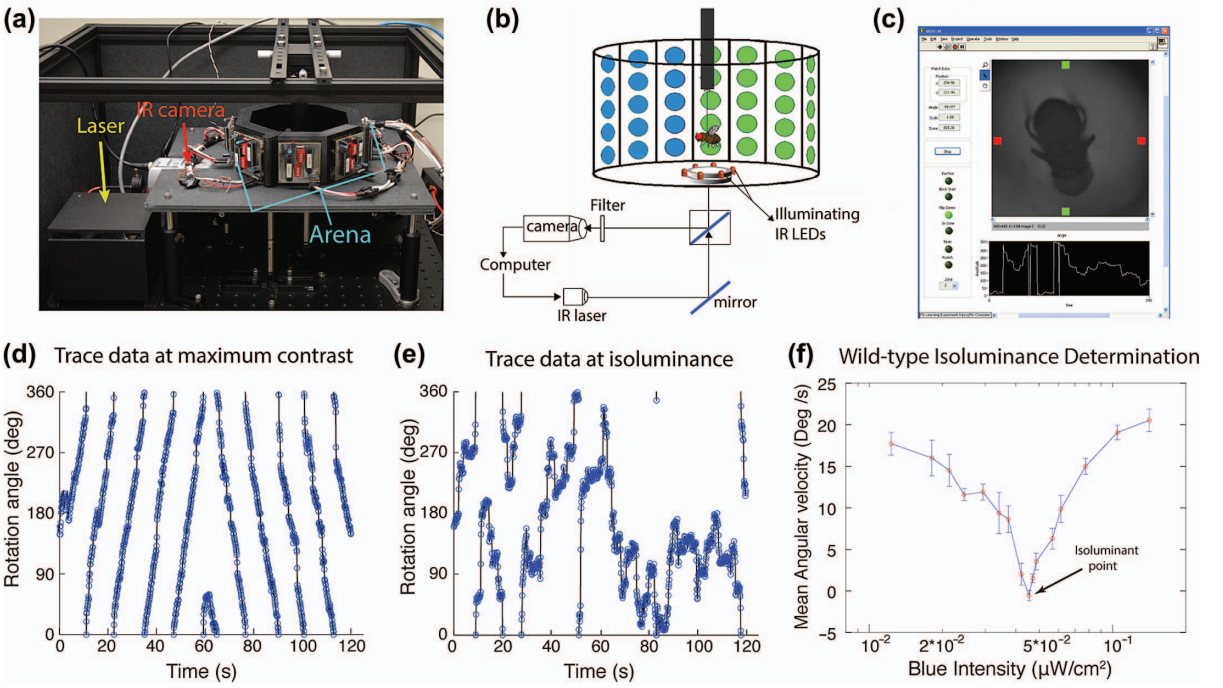

Figure 1. An aversive operant conditioning paradigm for true color vision. (**a**) Photograph of the flight simulator. An octagonal arena with blue (470 nm) and green (528 nm) LEDs allows for display of versatile visual stimuli, an infrared camera is used to monitor the fly's position, and a near-infrared laser is used to condition the fly with a heat beam. (**b**) Schematic of a tethered fly in the arena. A mirror and a beam splitter below the stage allow for a heat beam from the IR laser to be directed to the fly's abdomen and for reflected illuminating light from the fly to be directed to the camera. Custom software written in LabVIEW (screenshot in **c**) controls display of visual patterns, monitors the fly's position, and conditions the fly when appropriate. (**d–f**) Using the fly's optomotor response to determine the point of blue-green isoluminance. The fly's angular orientation is plotted as a function of time to generate a trace of the fly's optomotor response at maximum contrast (**d**) and at the isoluminant point (**e**). Flies are shown rotating patterns of alternating green bars of fixed intensity and blue bars of variable intensity. Plotting the average angular velocity of flies as a function of blue intensity (**f**) allows for determination of the blue-green isoluminant point, as the intensity that elicits minimal average angular velocity. Error bars = ± 1 SEM.

The following protocol was used to determine the isoluminance point. Flies were shown a rotating pattern of alternating green and blue stripes. The stripe width was 45°, the stimulus was rotated at 30°/s. For maximum contrast we used a pattern of alternating green and dark bars. To determine the point of isoluminance, we kept the green intensity fixed and varied the blue intensity (green fixed at 0.102 μW/cm^2 and the blue intensity varied between 0.01 and 0.14 μW/cm^2). For each intensity ratio, the stimulus was rotated for 1 minute clockwise, and 1 minute counterclockwise. The text output of the fly's position in each frame was analyzed in MATLAB (MathWorks, Natick, MA) to generate a plot of the fly's behavior in the 2-minute testing window. Syndirectional angular velocity was calculated by sampling the angular position every 300 ms, and averaging over the 2-minute period.

In the color entrainment experiment, flies were shown a pattern of alternating blue and green quadrants (width 90°), with the center two columns of each quadrant flashing to generate a flashing bar (width ~11°, frequency 2.5 Hz). The quadrants were rotated by 45° every 30 seconds. Lights were turned off for 1 second between each rotation of the visual panorama.

The intensities of the blue and green lights used in conditioning experiments were, at isoluminance, 0.058 μW/cm^2 (blue) and 0.102 μW/cm^2 (green) (designated b20 g20). The quantal flux at this isoluminant setting was 1.37×10^{11} quanta cm^{-2} s^{-1} (blue) and 2.71×10^{11} quanta cm^{-2} s^{-1} (green), which corresponded to a green/blue ratio of 1.98. We estimated the blue (470 nm)/green (528 nm) relative sensitivity of Rh1 to be 1.99 from the spectral sensitivity curve for Rh1 generated by Salcedo et al. (Salcedo et al., 1999, Figure 3) using voltage-clamp techniques. In the intensity-independence experiment, the corresponding intensities used for the brighter test condition was 0.131 μW/cm^2 (blue) and 0.102 μW/cm^2 (green) (designated b46 g20), which corresponded to a quantal flux of 3.09×10^{11} quanta cm^{-2} s^{-1} (blue) and 2.71×10^{11} quanta cm^{-2} s^{-1} (green). The conditioning paradigm was modified from Tang and Heisenberg (2004), and consisted of 8 blocks of time of about 2 minutes each, for a total of ˜17 minutes. The quadrants were thus rotated by four times in each 2-minute time block, thus covering all possible spatial orientations. The laser was turned on, and flies consequently conditioned with a near-IR laser in 4 of the 8 blocks. The conditioned zone was 80° wide, centered on the middle of the conditioned quadrant.

The laser power used was 650 mA. While in the conditioned zone, flies were punished for 400 ms, and given a break of 400 ms before being punished again. Flies' behavior in each 2-minute block was quantified by calculating a performance index (PI) = $[t_{safe} - t_{punish}]/t_{total}$. The PI of the test blocks was compared with the pretest by a two-tailed *t* test.

Mosaic Analyses and Immunohistochemistry

Single-cell mosaic experiments were carried out as described previously (Gao et al., 2008). Immunohistochemistry was performed as described previously (Ting et al., 2007). Confocal images were acquired using an upright Zeiss LSM780 microscope and deconvoluted using the Huygens Professional package (Scientific Volume Imaging, Hilversum, The Netherlands) running on a 64-core Fujitsu RX900 S1 with 1TB memory. The following concentrations of primary antibodies were used: mAb24B10 (1:100) (DSHB); rabbit mAb αGFP (1:400) (Invitrogen, Carlsbad, CA). The secondary antibodies including goat anti-rabbit and goat anti-mouse, coupled to Alexa488 and Alexa568, respectively (Molecular Probes, Eugene, OR) were used at a dilution of 1:400.

RESULTS

We constructed a magnetic tether based flight simulator (modified from Bender & Dickinson, 2006) for use in an aversive operant conditioning paradigm to entrain flies to discriminate hue (Figure 1a). In this paradigm, single flying flies are magnetically tethered in the center of an arena consisting of an octagonal array of 8×8 tricolor light-emitting diode (LED) panels (schematized in Figure 1b). Although the spatial resolution of the LED array is modest (~5.6 degree/pixel), the control board has been designed to provide precise intensity control (8-bit resolution) of green and blue LEDs. The fly is illuminated by infrared (IR) light; its position is continuously monitored using an IR camera. This apparatus allows us to both determine the point of blue-green isoluminance (see below) and entrain flies to discriminate between equiluminant blue and green stimuli. Custom software was written in LabVIEW (a screenshot is shown in Figure 1c) to display different visual patterns, track the flies' position in real time, and entrain them when appropriate using a near-IR laser for heat punishment.

Determining Blue-Green Isoluminance

Since motion vision in flies is known to depend on luminance contrast but not on hue (Yamaguchi et al., 2008), we used the flies' optomotor response to determine the point of blue-green isoluminance. Tethered flies shown a rotating pattern of alternating green and black bars (maximum contrast) exhibited a robust syndirectional optomotor response to this stimulus (representative trace is shown in Figure 1d). A close examination of their flight path revealed that flies by and large turned uniformly, with the occasional saccade (Figure 1d). The intensity of the green bar was kept fixed (at 0.102 μW/cm^2) and the blue intensity varied (between 0.01 and 0.14 μW/cm^2). At the isoluminant point, although flies changed their direction of flight several times in a 2-minute interval, there was no discernible pattern to their flight path (representative trace is shown in Figure 1e). Plotting the flies' average angular velocity as a function of different blue intensities allowed us to then determine the point of blue-green isoluminance (Figure 1f; the blue intensity at isoluminance was 0.058 μW/cm^2). In contrast to the strong optomotor response at maximum contrast (average angular velocity ~20°/s), the angular velocity at isoluminance was ~0°/s. The ratio of green (528 nm) to blue (470 nm) quantal flux at isoluminance was approximately 1.98, which corresponds well to the inverse of the estimated relative spectral sensitivity of the Rh1 opsin (1.99) to these wavelengths (Salcedo et al., 1999), and is consistent with a previous estimate of blue/green motion isoluminance ratio obtained using the head-yaw optomotor assay and a different light stimulus display (Huang & Lee, unpublished data). It is unclear, however, whether the electrophysiological measurements fully account for the effects of waveguide and visual pigments, which affect spectral sensitivity (Smakman & Stavenga, 1986). Together, these data are largely consistent with fly motion vision being largely mediated by Rh1 (Heisenberg & Buchner, 1977; Yamaguchi et al., 2008).

Wild-Type Flies Are Conditioned to Discriminate Blue From Green

We next used the above determined isoluminant intensities to entrain flies to avoid either blue or green, and thereby infer hue discrimination. The ~16-minute conditioning regimen (modified from Tang et al., 2004) was binned into eight 2-minute sessions, as schematized in Figure 2a. Flies were shown a pattern consisting of alternating blue and green quadrants with a flashing bar in the middle to attract flies to the center of the quadrant, and aversively conditioned with a heat beam from a near-IR laser to avoid either blue or green. The quadrants were rotated by 45° every 30 seconds (for a total of four times in a 2-minute session) to control for spatial cues (Figure 2a; see Methods for details). Thus, flies that maintained a steady heading in a 2-minute session would not exhibit a preference for either blue or green.

We started by examining the flight path of wild-type flies in this operant conditioning paradigm (a representative trace is shown in Figure 2a). In the pretest period,

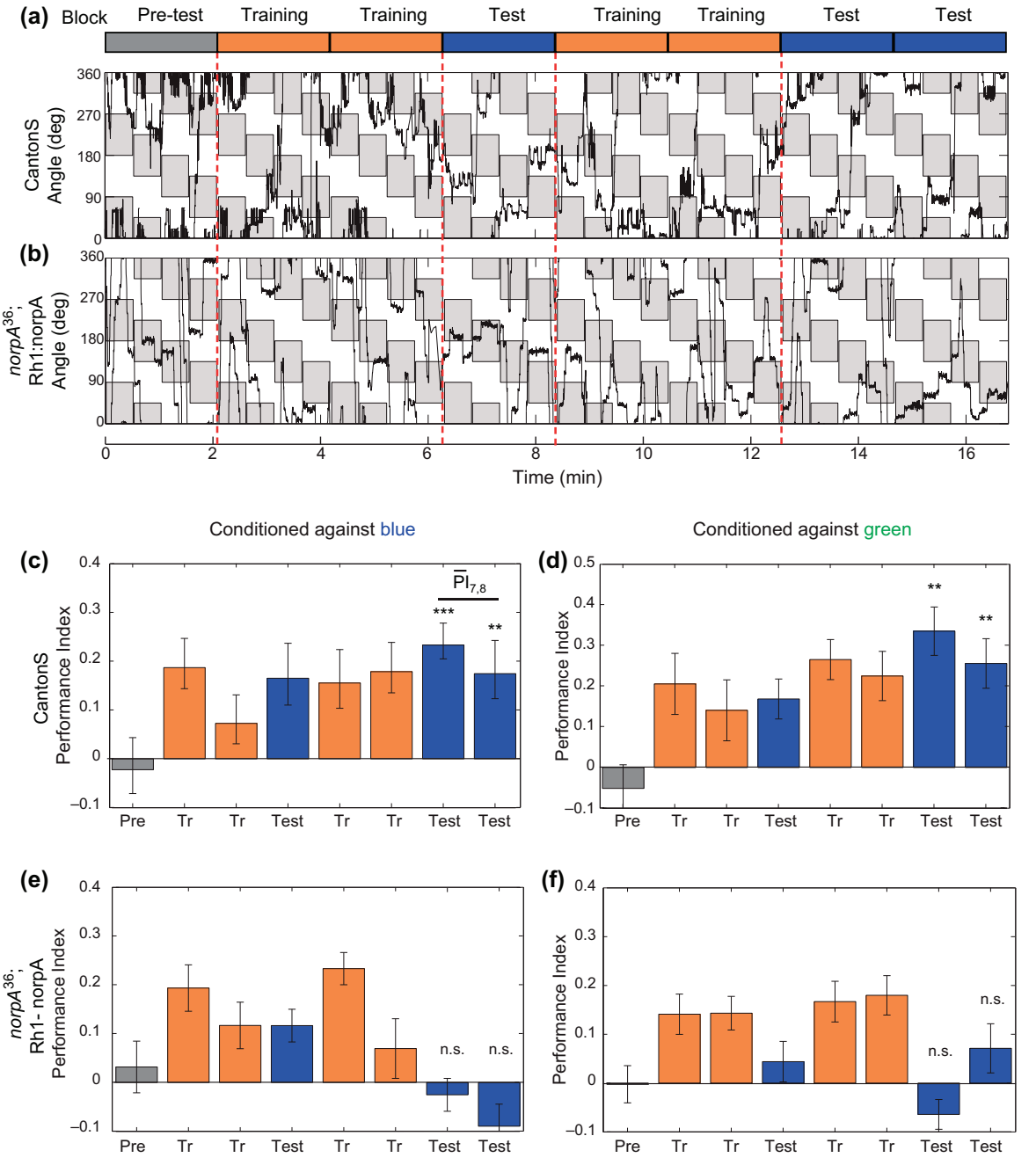

Figure 2. Blue-green color entrainment requires the functions of the inner photoreceptors R8 and/or R7. (**a**) Trace data of wild-type flies conditioned against blue. Flies are shown a stimulus consisting of alternating equiluminant blue and green quadrants that are rotated by 45° every 30 seconds. The fly's angular orientation is plotted as function of time; quadrants where the fly is punished are shaded in gray. In this experiment the gray blocks in the figure correspond to green quadrants in the arena, and white blocks to blue quadrants. The rotation of the quadrants is thus represented by the periodic change in orientation of the gray patches. The conditioning regimen is schematized above, the laser is turned on in the training blocks to condition flies, but kept off in the test and pretest blocks. (**b**) Trace data of Rh1-rescued flies conditioned against blue. R1–R6 function was rescued by expressing the phospholipase C *norpA* under the control of a Rh1 promoter, in a *norpA*-null mutant background. (**c**–**f**) Bar plots of the performance index (PI) of wild-type (**c**, **d**) and Rh1-rescued (**e**, **f**) flies conditioned against blue (**c**, **e**) or green (**d**, **f**). In contrast to wild-type flies, performance of Rh1-rescued flies in the test periods was not significantly different from pretest, indicating that Rh1 function is not sufficient for color entrainment. Bars are color coded as per the schematic in (**a**). PI of the test blocks was compared with the pretest by a two-tailed *t* test. $^{***}P < 0.001$; $^{**}P < 0.01$; n.s., not significant ($P > 0.05$). Average of the two test blocks was computed ($\overline{PI7,8}$) for each condition. Genotypes: *CantonS* (wild-type), *norpA*^{36}; *Rh1-norpA* (Rh1 rescued). $n = 19$–21 flies per condition. Error bars = ± 1 SEM.

wild-type flies did not exhibit a significant preference for either blue or green quadrants. We note, however, that the flies did not simply maintain a fixed heading through this pretest period, but instead appeared to frequently alter their course of heading and consequently dwell in the four quadrants of the visual panorama. Flies appeared to track both the flashing bar presented at the center of each quadrant, and the chromatic edge between blue and green quadrants. During the training sessions, flies avoided the punished zones, and dwelled longer in the "safe" zones. Flies continued to avoid the punished zones and prefer the safe zones in the posttraining test sessions when the laser was off. The periodic rotation of the orientation of the punished zones ensured that flies did not associate punishment with a specific spatial orientation. One concern that remained, though, is that flies might not associate punishment with the stimulus per se, but instead learn an "escape path" that allows them to avoid punishment, which is then simply repeated in the test sessions. However, flies' flight paths were different both between separate training sessions, and between training and test sessions, indicating that conditioning did not simply induce a repetitive flight pattern, but instead the flies learned to discriminate the two stimuli, and choose the "safe" zone.

Flies' choices were quantified by calculating a performance index (PI) for each 2-minute bin as the time spent in safe quadrants minus the time spent in the punished quadrants divided by the total time. An average PI was then computed for ~20 flies per condition. As suspected from visual examination of the flight trace, wild-type flies conditioned against blue on average, exhibited no innate preference for blue or green (mean pretest PI, $\overline{PI1} = 0.02$), but showed a robust bias towards green after training (mean test PI, $\overline{PI7,8} = 0.204$, $P < 0.003$; Figure 2c). Similarly, flies conditioned against green had no significant preference for blue or green ($\overline{PI1} = -0.05$, not significantly different from 0), but after training developed a robust preference for blue ($\overline{PI7,8} = 0.294$, $P < 0.003$; Figure 2d). Thus, flies can be successfully entrained to avoid either blue or green by operant conditioning, their learned response to conditioning being characterized by a PI of ~0.2–0.3 (hereafter referred to as "normal learning").

Output of Narrow-Spectrum Photoreceptors R8 and/or R7 Is Required For Color Entrainment

If flies were using hue to discriminate between the blue and green stimuli, we would predict that this discrimination ability would require the functions of the narrow-spectrum inner photoreceptors R8 and/or R7, as true color vision requires comparison of at least two photoreceptor classes. To test this prediction, we generated flies where the phospholipase C *norpA* (essential for phototransduction) function was restored with a Rh1 promoter in a *norpA* mutant background (*norpA*^{36}; Rh1-*norpA*). In these flies (hitherto referred to as "Rh1-rescued" animals), the outer photoreceptors R1–R6 were the only functional photoreceptor class. The blue-green isoluminant point for these Rh1-rescued animals, as determined by the optomotor response, was the same as for wild-type flies (data not shown), consistent with fly motion vision being primarily mediated by R1–R6 (Yamaguchi et al., 2008). Examination of their flight path in the conditioning paradigm (representative trace in Figure 2b) showed that like wild-type flies, Rh1-rescued flies also exhibited no evident preference for blue or green quadrants in the pretest and avoided the punished zones in the training sessions. However, unlike wild-type flies, the Rh1-rescued animals did not show a preference for the "safe" zones in the test sessions following the training sessions. We note that the behavior of the Rh1-rescued flies in test periods was characterized by many changes of flight direction and by their dwelling in both safe and punished zones without significantly preferring either as opposed to merely maintaining a fixed heading (which would have also resulted in no net preference). On average, Rh1-rescued flies conditioned against blue (Figure 2e) did not exhibit a significant preference for blue or green in pretest sessions ($\overline{PI1} = 0.032$); the PI in test sessions was not significantly different from the pretest ($\overline{PI7,8} = -0.058$, $P > 0.06$). Similar results were obtained when Rh1-rescued flies were conditioned against green ($\overline{PI1} = -0.002$, $\overline{PI7,8} = 0.004$, $P > 0.1$; Figure 2f). Thus, restoring the function of the Rh1 channel in a blind fly was insufficient for color entrainment, indicating that, as predicted, R8 and/or R7 function is required in our blue-green color discrimination task. Since color vision is known to require the output of multiple photoreceptors of differing spectral sensitivities, this result that a single broad-spectrum photoreceptor channel is insufficient for color learning supports the idea that blue-green discrimination in our entrainment assay is mediated by a color vision–like system in *Drosophila*.

Color Entrainment Is Intensity Independent in a 2-Fold Intensity Range

True color vision is defined as hue discrimination independent of intensity, at least within a limited range. Therefore, we would predict that if flies were indeed using hue to discriminate between the blue and green quadrants in our assay, this discrimination ability would persist even when the intensities of blue and green differed between the test and training periods. We modified the conditioning regimen in order to test this prediction (schematized in Figure 3a). Wild-type flies were entrained at the above determined isoluminant intensities (designated b20 g20), but tested at a higher intensity (designated b46 g20). We note that flies presented with rotating pattern of green

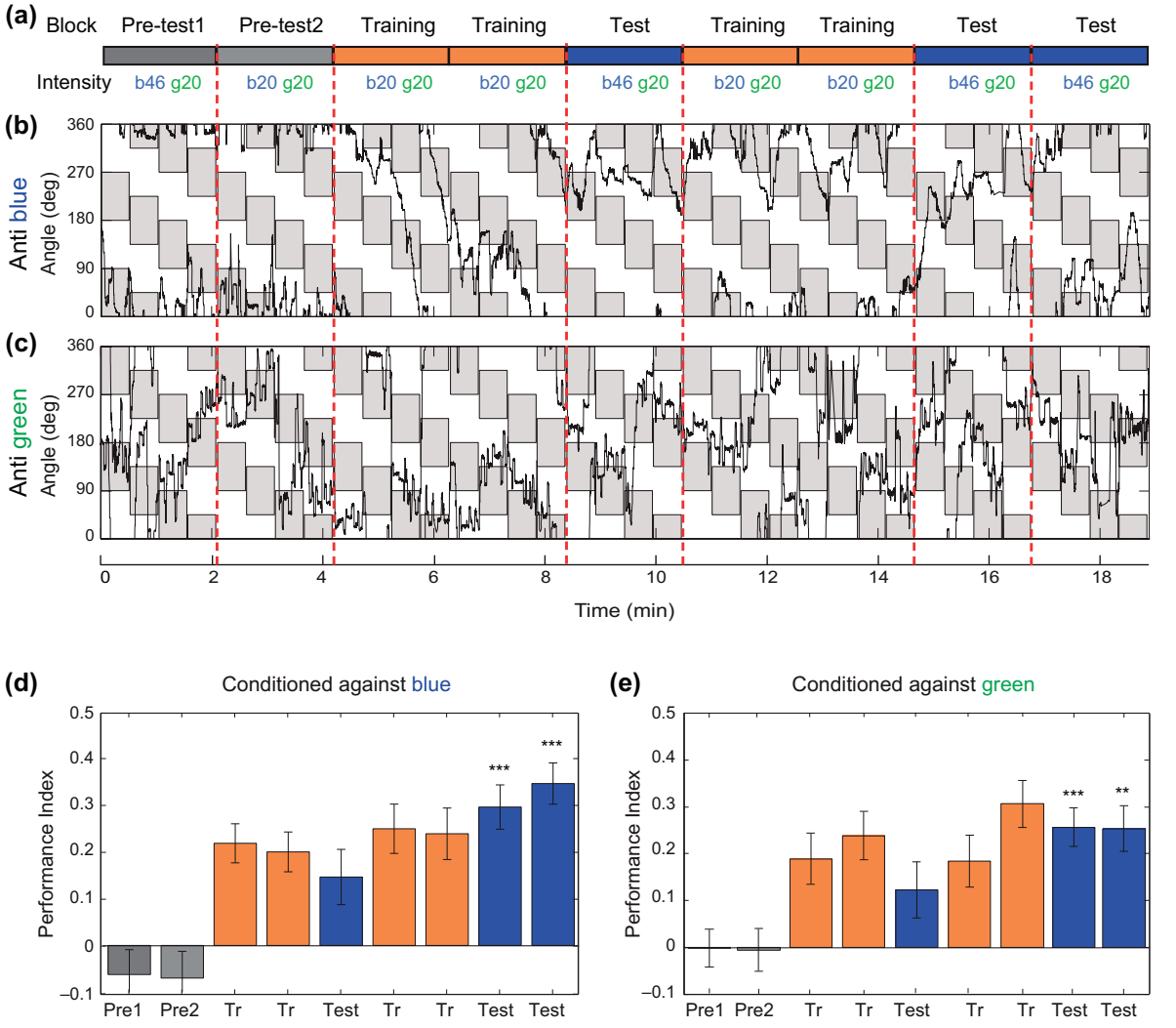

Figure 3. Color entrainment is intensity independent in a 2-fold intensity range. (**a**) Schematic of the training paradigm for testing intensity independence. Flies were trained at equiluminant blue and green intensities (b20 g20), but tested at a brighter blue intensity (b46 g20). (**b**–**c**) Trace data of wild-type (CantonS) flies conditioned against blue (**b**) or green (**c**) in the intensity independence paradigm. Visual stimulus display is as in Figure 2a. As in Figure 2a, the fly's angular orientation is plotted as function of time; quadrants where the fly is punished are shaded in gray. Gray-shaded blocks in **b** correspond to green quadrants in the arena, and to blue quadrants in **c**. (**d**–**e**) Bar plots of wild-type flies conditioned against blue (**d**) or green (**e**). Flies retained the ability to discriminate blue from green when they were challenged with the brighter blue, indicating that learning is intensity independent in this intensity range. PI of the test blocks was compared with the pretest for the higher blue intensity by a two-tailed *t* test. $^{***}P < 0.001$; $^{**}P < 0.01$.

and blue bars at this higher intensity exhibited a robust optomotor response (Figure 1f), indicating that flies were able to discern this difference in intensity. On average, flies conditioned against blue using this protocol, retained a very highly significant avoidance of the brighter blue zones, and consequent preference of the "safe" green zones, after training (mean test $\overline{\mathrm{PI}} = 0.32$, vs. $\overline{\mathrm{PI1}} = -0.06$, $P < 0.0001$; Figure 3d). Similar results were obtained when flies were conditioned against green (mean test $\mathrm{PI} = 0.26$ vs. $\mathrm{PI1} = -0.01$, $P < 0.004$; Figure 3e). Representative traces of flies' angular position are shown for flies conditioned against blue (Figure 3b) or green (Figure 3c). Color entrainment in our assay thus requires the output of narrow-spectrum photoreceptors, and appears to be, at least within a very limited 2-fold range, intensity independent, thus meeting two requirements of an assay for true color vision.

Blocking the Output of the Tm5a/b/c and Tm20 Neurons Disrupts Color Discrimination

Having established that entrainment in our assay is mediated by a color vision system in *Drosophila*, we next sought to determine the substrates that implement this system. Since the inner photoreceptors R8/R7 appear to be required for color entrainment in our assay, we focused

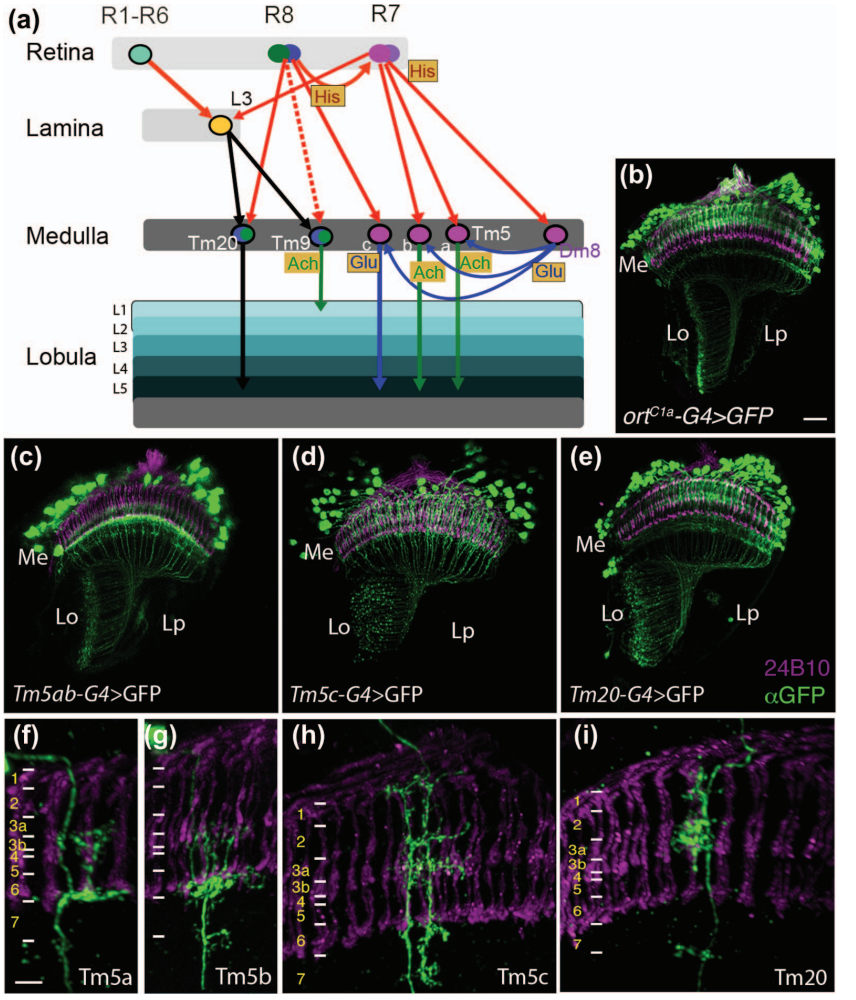

Figure 4. Visual circuits downstream of chromatic photoreceptors. (**a**) Schematic of currently known visual circuits, highlighting the neurons known to receive input from multiple photoreceptors. Neuronal cell bodies are denoted by ovals. Arrows indicate axonal projections, a solid arrow between two neurons indicates a chemical synapse validated by electron microscopy, and a dashed arrow indicates a chemical synapse determined using GRASP (GFP Reconstitution Across Synaptic Partners; Feinberg et al., 2007; Gordon & Scott, 2009; Karuppudurai et al., 2014). Arrows are color coded according to the neurotransmitter system expressed in the particular neuronal type. Thus, histaminergic projections from the photoreceptors are red, glutamatergic projections are blue, cholinergic projections are green, and axonal projections of an undetermined neurotransmitter type are black. Neurotransmitter systems expressed in particular cell types are also marked in shaded boxes. Ach = acetylcholine; Glu = glutamate; His = histamine. (**b**–**i**) Confocal images of adult optic lobes stained with mAb24B10 (magenta) to label photoreceptors and therefore mark medulla column positions, and an anti-GFP antibody to mark target neuron projections. (**b**) ort^{C1a}-GAL4 > UASmCD8GFP. (**c**–**e**) ort^{C1a}-GAL4 DBD crossed to different dVP16AD lines to generate subtype-specific lines. (**c**) ort^{C1a}-GAL4DBD; 24g-dVP16AD. Single-cell flip-out clones identify labeled cells in this line as Tm5a (**f**) and Tm5b (**g**). (**d**) ort^{C1a}-GAL4DBD / OK371-dVP16AD. Single-cell flip-out clones indicate that this driver combination labels largely Tm5c neurons (**h**). (**e**) ort^{C1a}-GAL4 DBD / ET9A-dVP16AD. Single-cell flip-out clones indicate that this driver combination labels largely Tm20 neurons (**i**). Scale bars: 20 μm in **b** for **c**–**e**; 5 μm in **f** for **g**–**i**. Positions of medulla layers are marked in **f**–**i**.

on the medulla projection neurons that are downstream of R8 and/or R7. Our previous work (Gao et al., 2008, Karuppudurai et al., 2014) determined that the Tm20, Tm9, and Tm5a/b/c medulla projection neurons express the histamine chloride channel receptor *ora transientless* (*ort*), making them excellent candidates. Figure 4a schematizes what is currently known about their connectivity and neurotransmitter usage (derived from Gao et al., 2008; Karuppudurai et al., 2014; Takemura et al., 2013).

Of these five classes of neurons, we focused on Tm5a/b/c and Tm20, as they project to deeper layers of the lobula neuropil (Lo5 and 6), which are suspected to mediate color vision in analogy to honeybees (reviewed in Dyer et al., 2011). Tm9, in contrast, projects to T5 neurons at the superficial layer of the lobula (Lo1) and feeds into the motion detection pathway (Shinomiya et al., personal communication). Using comparative genomics, we previously identified a conserved region

of the *ort* enhancer termed *ort*^{C1a} that drives expression in the Tm5a/b/c and Tm20 neurons (Karuppudurai et al., 2014). Therefore, to silence synaptic transmission in the Tm5a/b/c and Tm20 neurons, and thereby determine if their output is functionally required for color entrainment, we used the *ort*^{C1a} promoter to express the tetanus toxin light chain (TNT; which cleaves synaptobrevin) in these neurons so as to block their synaptic transmission (Sweeney et al., 1995). The *ort*^{C1a}*-GAL4 UAS-TNTE* flies exhibited defective UV spectral preference behavior, indicating that this manipulation was effective in blocking synaptic transmission (Karuppudurai et al., 2014). These flies exhibited a robust optomotor response in our optomotor assay, however, with the same blue-green isoluminant point as wild-type flies, indicating that these animals were not generally defective in visual function (data not shown). However, these animals did not modulate their blue-green preference in response to conditioning against blue ($\overline{PI7,8} = 0.095$ vs. $\overline{PI1} = 0.054$, $P > 0.33$) or green ($\overline{PI7,8} = 0.045$ vs. $\overline{PI1} = -0.023$, $P > 0.29$) (Figure 5a), implying that chemical transmission from these neurons was required for normal color entrainment. Supporting this conclusion, *ort*^{C1a}*-lexADBD*::*VP16AD*/*LexAop-TNT::HA* animals were also defective in color learning (Figure 5a). In contrast, *ort*^{C1a}*-GAL4* animals exhibited normal learning, indicating that the phenotype we observed in *ort*^{C1a}*-GAL4 UAS-TNTE* flies was not attributable to the genetic background of the *ort*^{C1a}*-GAL4* line (Figure 5a). Two-way analysis of variance (ANOVA) confirmed that the learning scores of Rh1-rescued, *ort*^{C1a}*-GAL4 UAS-TNTE*, and *ort*^{C1a}*-lexADBD*::*Vp16AD*/*LexAop-TNT::HA* flies were not statistically different from each other ($P > 0.05$) but were significantly different from learning scores of wild-type and *ort*^{C1a}*-GAL4* control flies ($P < 0.05$), which were in turn not statistically different from each other. The learning scores thus distributed into two groups—the "wild-type" group containing CS and *ort*^{C1a}*-GAL4* control flies and the "mutant" group consisting of Rh1-rescued, *ort*^{C1a}*-GAL4 UAS-TNTE*, and *ort*^{C1a}*-lexADBD*::*Vp16AD*/*LexAop-TNT::HA* flies—characterized by statistically significant differences between groups but not within groups. Taken together, these data minimally imply that the output of one or more of Tm5a/b/c and Tm20 neurons is required for color entrainment.

We next attempted to genetically dissect the relevant projection neuron classes for color entrainment behavior, by driving TNT expression in subsets of Tm5a/b/c, and Tm20 neurons (Figure 5b). Tm20 seemed to be an attractive candidate to mediate blue-green color vision, as it is a major downstream target of the blue-green photoreceptor R8 (Takemura et al., 2013). We used the combinatorial split-GAL4 system (Luan et al., 2006) to restrict the expression of the *or*^{C1a} promoter to subsets of medulla neurons. In this system, the GAL4 DBD fused to a dimerization motif, and the activation domain (AD) also fused to a dimerization motif, are expressed under the control of different enhancers that have overlapping, but distinct expression patterns. Intact GAL4 would thus be reconstituted only in regions where the enhancer expression patterns overlap. Thus, we crossed the *ort*^{C1a} GAL4 DBD flies to a number of enhancer trap *VP16AD* lines to generate combinatorial driver lines that specifically drive expression in Tm5a/b, Tm5c, and Tm20 neuronal subtypes (Figure 4b–i; Karuppudurai et al., 2014; Ting et al., 2014). However, *Tm20-GAL4 UAS-TNTE* animals (Ting et al., 2014) (see Methods for genotypes) exhibited normal learning (Figure 5b). Similar results were obtained with *Tm20-LexA*/*LexAop-TNT::HA* flies, indicating that the output of Tm20 is not exclusively required for color entrainment. We therefore proceeded to test if the output of Tm5a/b/c neurons was required by crossing the *UAS-TNTE* line to *Tm5abc-GAL4*. Surprisingly, however, these *Tm5abc-GAL4 UAS-TNTE* animals also exhibited normal learning (Figure 5b), implying that the output of the Tm5a/b/c neurons was also not exclusively required for color learning. The same treatment abolished UV spectral preference behavior, indicating that this treatment was effective in blocking transmission in these neurons (Karuppudurai et al., 2014). Taken together, these data suggest that color entrainment requires the activity of one or more of the Tm5a/b/c neuronal classes in a redundant fashion with Tm20.

We therefore next examined the behavioral consequences of silencing synaptic transmission in Tm5c and Tm20 neurons. These *Tm5c + 20-GAL4 UAS-TNTE* flies, however, exhibited normal learning, as did *Tm5ab + 20-GAL4 UAS-TNTE* flies (Figure 5b). We used the same *UAS-TNTE* transgene that was used with the *ort*^{C1a}-GAL4 with all the subtype-specific GAL4s (Figure 5a); the fact that we didn't observe a color learning phenotype with any of the subtype-specific GAL4 lines indicates that the entrainment phenotype we observed in *ort*^{C1a}*-GAL4 UAS-TNTE* flies was not ascribable to the genetic background of this line. Taken altogether, these data suggest that functional color discrimination requires the output of the Tm5a/b, Tm5c, and Tm20 neurons in a redundant manner. In turn, this would imply that any the output of any one of the Tm5a/b, Tm5c, and Tm20 neurons is sufficient to mediate functional color discrimination.

DISCUSSION

Here, we show that *Drosophila* possesses a color vision system, and demonstrate that functional color discrimination requires the redundant function of four classes (three groups) of medulla projection neurons. To test true color vision in *Drosophila*, we developed a novel aversive operant conditioning assay. Wild-type flies were successfully trained in this paradigm when conditioned against

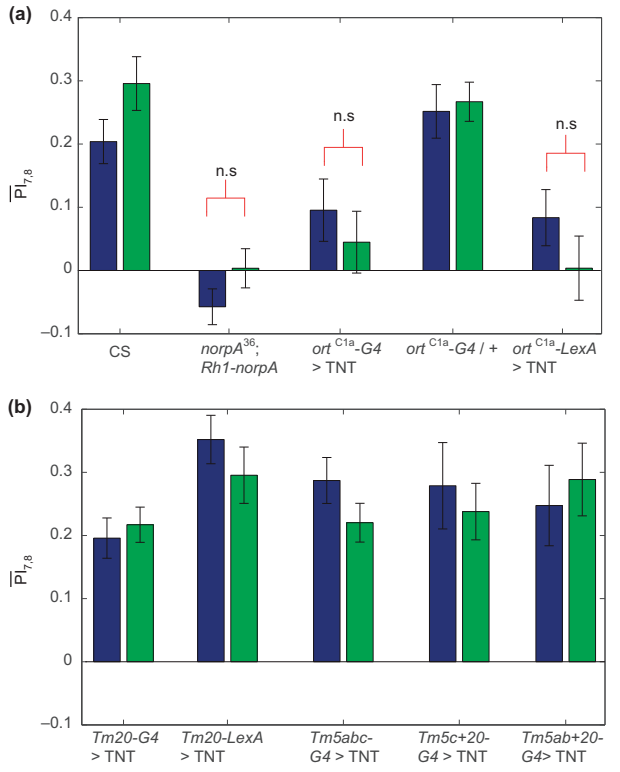

Figure 5. Tm5a/b, Tm5c, and Tm20 neurons likely redundantly mediate learned color discrimination. Requirement of specific neurons for color entrainment was evaluated by examining performance of flies expressing tetanus toxin (TNT) to block synaptic transmission, under the control of different medulla neuron-specific lines. Bar plots show mean test PI ($\overline{PI7,8}$) of flies of indicated genotypes. Bars are color coded according to the color flies were conditioned against. Significance was evaluated by comparing test PI to pretest for each condition. (**a**) *ort*^{C1a}-expressing neurons are required for color entrainment. Expressing TNT with this promoter using either the GAL4 or the LexA system abolished learning in contrast to controls. (**b**) Blocking function of Tm20 alone, or any two of Tm5a/b, Tm5c, and Tm20 classes, is insufficient to block color entrainment. In contrast to the result in **a** above, learning scores were in the wild-type range ($\overline{PI7,8}$ = ~0.2–0.3) for these subtype-specific manipulations, suggesting that Tm5a/b, Tm5c, and Tm20 redundantly mediate color entrainment. All scores are highly significant ($P < 0.01$) unless otherwise noted. n.s. = not significant ($P > 0.05$), $n = 17$–21 flies per condition for all genotypes except Tm5ab + 20 and Tm5c + 20 ($n = 8$–9 flies per condition). Error bars = ± 1 SEM.

either green or blue. The narrow-spectrum photoreceptors R8 and/or R7 were required for color entrainment. Furthermore, this entrainment behavior was intensity independent within a narrow 2-fold range, thus meeting two criteria for true color vision. Inactivating chemical transmission in the Tm5a/b, Tm5c, and Tm20 medulla projection neurons collectively abolished learning, whereas inactivation of Tm20 alone or any two of these classes was insufficient to block entrainment. Thus, blue-green color discrimination likely requires the redundant function of Tm5a/b, Tm5c, and Tm20 projection neurons, suggesting that color is represented along multiple redundant axes in the fly's medulla.

A Novel Assay for Fly Color Vision

Drosophila exhibits a range of wavelength-discrimination behaviors, with a particularly strong innate preference for UV over visible light (Fischbach, 1979; Gao et al., 2008; Yamaguchi et al., 2010). Responses of flies in these assays, however, depended on both the wavelength and intensity of light, making them unsuitable as tests of true color vision. True color vision has been operationally defined as the ability to discriminate lights/surfaces based on spectral properties (i.e., discriminate hue independent of intensity; Wyszecki & Stiles, 1982). It has traditionally been demonstrated in animals using conditioning (Kelber et al., 2003), in part because a learned response is thought to require an internal neural representation of color (Menzel, 1979; Goldsmith, 1991). Therefore, we constructed a modified flight simulator (Bender & Dickinson, 2006) for use in an aversive operant conditioning paradigm for fly color entrainment. With this apparatus, we were able to first determine with a high degree of precision the point of blue-green isoluminance, using the fly's optomotor response, and then condition the fly to avoid equiluminant blue and green stimuli. The flies in our paradigm had no innate preference for blue or green on average, but developed a robust preference for the "safe" color post entrainment. Their behavior in the test phases was characterized by a performance index (PI) of 0.2–0.3, which corresponds well with the behavioral criteria established for learned wavelength discrimination in butterflies (Koshitaka et al., 2008).

This learned preference we obtained in our assay is higher than those obtained using classical associative color conditioning paradigms (Menne & Spatz, 1977; Hernández de Salomon & Spatz, 1983; Schnaitmann et al., 2010). The design of our assay differs from these efforts in a few important ways. First, using the same apparatus we use for conditioning, we are able to reliably and accurately determine the blue-green isoluminant point, ensuring that flies in our assay show no significant preference for blue or green preentrainment. Second, we rotate the orientation of the green and blue quadrants every 30 seconds, averaging the flies' choices over a 2-minute window to determine an average PI. Thus, for flies to be scored as having a significant preference, they would have to make several choices to change their orientation in the test periods, giving us greater confidence that our results accurately represent flies' choice behavior. Third, our assay uses tethered flight behavior, whereas previous work utilized walking behavior. Changes in behavioral state might contribute to differential tuning sensitivity, as shown for motion detection (Chiappe et al., 2010). The associative conditioning

studies trained flies in large groups, however, and therefore offer the advantage of high throughputs and ability to test large number of flies compared with our individual tethered fly assay.

Drosophila Possesses A Color Vision System

Since true color vision requires comparison of the outputs of more than one class of photoreceptor, we reasoned that if our assay were indeed a test of true color vision, flies with only one active class of photoreceptors should fail to discriminate blue and green in our assay. We therefore restored *norpA* function with a *Rh1* promoter in a $norpA^{36}$-null mutant background, to generate flies with the broad-spectrum R1–R6 as the only functional photoreceptors. These flies showed no significant learning in our assay, implying that blue-green color entrainment requires the function of the narrow-spectrum photoreceptors R8 and/or R7. This result is consistent with work in blowflies (Troje, 1993) and recently in *Drosophila* (Schnaitmann et al., 2013). Schnaitmann et al. (2013) report that the photoreceptors R1–R6 contribute to fly color entrainment likely via the lamina neurons L2 and/or L1. This is perhaps surprising, as the L1/L2 pathway is known to mediate motion detection (Clark et al., 2011; Joesch et al., 2010; Rister et al., 2007), and there is scarce anatomical evidence that the pathway contributes to integration of input from more than one photoreceptor class. It is unclear whether behavioral state, i.e., walking vs. flying, contributes to this unexpected requirement. However, we are unable to test for the requirement of L1/L2 for color discrimination in our assay, as we use the flies' optomotor response to determine the isoluminant point. In so using the optomotor response to set the isoluminant point, we have in effect balanced the Rh1 input into the fly's putative color vision system, and are measuring effects of circuit perturbations in this background.

A further requirement of blue-green discrimination in our assay being mediated by a color vision system is that the discrimination is independent of the intensity of the blue and green stimuli. Indeed, flies in our assay robustly modulated their blue-green preference even when they were tested at a brighter blue intensity than the equiluminant blue and green intensities they were entrained with. Blue-green entrainment in our assay is thus likely mediated by a color vision system in *Drosophila*.

Tm5a/b, Tm5c, and Tm20 Likely Redundantly Mediate Color Vision

The narrow-spectrum photoreceptors R8 and R7 project to the medulla and connect to specific medulla projection neurons and amacrine cells. Here, we focused on the medulla projection neurons Tm20, Tm5c, and Tm5a/b, as they are known to be downstream of R8 and R7 and project to deeper layers (Lo5/6) of the lobula. In addition, Tm20 and Tm5c also receive indirect input from the broad-spectrum photoreceptors R1–R6 via the lamina neuron L3. These neurons thus receive input from multiple classes of photoreceptors, and are therefore excellently positioned to mediate a color vision system. Blocking chemical transmission in the Tm5a/b/c and Tm20 neurons abolished learning, indicating that color entrainment required the function of these three classes. However, blocking transmission of any two of these three classes had no effect on color entrainment. This result might be explained as a consequence of lower levels of transgene expression in the class-specific driver lines resulting from our using the split GAL4 system to generate these lines. We note, however, that the split lines use the *dVP16AD* activation domain, which drives a higher level of expression than the GAL4 activation domain. Further blocking synaptic transmission using the Tm5c-GAL4 was sufficient to block UV preference behavior, a behavioral effect that was not different from that obtained with the ort^{C1a}-*GAL4* line (Karuppudurai et al., 2014). Thus, the difference in color learning behavior outcomes we see between the ort^{C1a}-*GAL4* and the subtype-specific GAL4 lines is unlikely to be explained by differences in levels of transgene expression. Instead, our results are consistent with the idea that Tm5a/b, Tm5c, and Tm20 are redundantly required for color entrainment. In turn, this suggests that the function of any one of these three pathways is sufficient for color entrainment. Since these neurons are known to receive inputs from R1–R6, R7, and R8 (Figure 4a), this result is in agreement with and complements the recent report that multiple combinations of the Rh1, Rh4, and Rh6 photoreceptor channels are sufficient to mediate color entrainment (Schnaitmann et al., 2013).

Learned Color Discrimination Utilizes Multiple Redundant Pathways, in Contrast to Innate Spectral Preference Behavior

Our finding that multiple redundant projection neuron classes mediate color entrainment contrasts sharply with the single pathway that dominates innate UV spectral preference behavior (Gao et al., 2008; Karuppudurai et al., 2014). Flies' innate UV preference is mediated by a pooling circuit: single wide-field Dm8 neurons pool input from ~16 R7 photoreceptors in its receptive field, and output to one columnar Tm5c neuron at the center of its dendritic field (Gao et al., 2008; Karuppudurai et al., 2014). Tm5c but not Tm5a/b (which also receive Dm8 input) neurons are required for UV spectral preference behavior. Flies thus appear to represent color along multiple redundant axes at this first synapse in the visual system, whereas

innate spectral preference utilizes a single pathway (i.e., R7s-Dm8-Tm5c). Utilizing multiple redundant pathways for learned color discrimination might offer organisms the advantage of being able to tune the weights of different channels to meet their ecological needs.

Primate retinal ganglion cells (anatomically analogous to insect medulla projection neurons) represent color information along multiple spectrally opponent axes, and are thought to be the neural implementation of the second stage of color processing (Calkins & Sterling, 1999). Although their role in functional hue discrimination remains undetermined, this suggests that color representation along multiple axes might be a common feature of visual systems. Based on the available connectivity diagram (Figure 4a; Gao et al., 2008; Takemura et al., 2013), it remains to be determined whether some or all of the four Tm neurons characterized here are capable of serving as color opponent neurons. Tm20 receives both direct inputs from R8 photoreceptors and indirect input from R1–R6 via L3, but the nature of this convergence is not known. Alternatively, R8 and R7 are known to synapse on each other and spectral opponency in *Drosophila* could arise at the level of the photoreceptors themselves, as suggested previously for butterflies (Takemura et al., 2008; Takemura & Arikawa, 2006). Primate S cones have recently been shown to get opponent inputs from horizontal cells (Packer et al., 2010; Dacey et al., 2013) and generate blue-yellow opponent responses, whereas in ground squirrels, a specific amacrine type provides a blue-OFF signal to the blue-yellow opponent ganglion cells (Chen & Li, 2012). Alternatively, spectral opponency could arise downstream of these medulla projection neurons, or these cells might implement spectral preprocessing filters that are hypothesized to form the basis of simple color constancy (van Hateren, 1993). Differentiating between these possibilities must await electrophysiological or functional imaging studies on these Tm neurons and the characterization of their chromatic tuning properties.

In summary, this work represents the first demonstration that specific classes of visual neurons are required for functional hue discrimination. Activity measurements in these neurons will allow us to determine the computations they perform, and begin to understand how color percepts in deeper brain regions derive from photoreceptor activation patterns in the eye.

ACKNOWLEDGMENTS

We thank Martin Heisenberg for suggestions on behavioral assays, Michael Reiser and Mark Frye for help with the magnetic tethering system, Craig Montell and Benjamin White for fly lines, and Claude Desplan and Nina Vogt for communicating results prior to publication. This work was supported by the Intramural Research Programs of the NIH, *Eunice Kennedy Shriver* National Institute of Child Health and Human Development (grant Z01-HD008776 to C.-H.L) and Center for Information Technology (R.P. and T.P.), and the intramural funds of the National Institute of Biomedical Imaging and Bioengineering (P.D.S.).

Declaration of interest: The authors report no conflicts of interest. The authors alone are responsible for the content and writing of the paper.

REFERENCES

Borst, A. (2009). *Drosophila*'s view on insect vision. *Curr Biol, 19,* R36–R47.

Bender, J. A., & Dickinson, M. H. (2006). Visual stimulation of saccades in magnetically tethered *Drosophila*. *J Exp Biol, 209* (Pt 16)*,* 3170–3182.

Cajal, S. R., & Sanchez, D. (1915). Contribucion al conocimiento de los centros nerviosos del los insectos. *Trab Lab Invest Biol, 13,* 1–167.

Calkins, D. J., & Sterling, P. (1999). Evidence that circuits for spatial and color vision segregate at the first retinal synapse. *Neuron,* 24*,* 313–321.

Chen, S., & Li, W. (2012). A color-coding amacrine cell may provide a blue-off signal in a mammalian retina. *Nat Neurosci, 15,* 954–956.

Chiappe, M. E., Seelig J. D., Reiser, M. B., & Jayaraman, V. (2010). Walking modulates speed sensitivity in *Drosophila* motion vision. *Curr Biol, 20,* 1470–1475

Clark, D. A., Bursztyn, L., Horowitz, M. A., Schnitzer, M. J., & Clandinin, T. R. (2011). Defining the computational structure of the motion detector in *Drosophila*. *Neuron, 70,* 1165–1177.

Crane, J. (1955). Imaginal behavior of a Trinidad butterfly, Heliconius erato hydara Hewitson, with a special reference to the social use of color. *Zoologica, 40,* 167–196.

Dacey, D. M. (2004). Origins of perception: Retinal ganglion cell diversity and the creation of parallel visual pathways. In M. S. Gazanniga (Ed.), *The cognitive neurosciences* (pp. 281–301). Cambridge, MA: MIT Press.

Dacey, D. M., Crook, J. D., & Packer, O. S. (2013). Distinct synaptic mechanisms create parallel S-ON and S-OFF color opponent pathways in the primate retina. *Vis Neurosci,* 1–13.

Duistermars, B. J., & Frye, M. A. (2008). A magnetic tether system to investigate visual and olfactory mediated flight control in *Drosophila*. *J Vis Exp, 21,* e1063.

Dyer, A. G., Paulk, A. C., & Reser, D. H. (2011). Colour processing in complex environments: Insights from the visual system of bees. *Proc Biol Sci, 278,* 952–959.

Feinberg, E. H., Vanhoven, M. K., Bendesky, A., Wang, G., Fetter, R. D., Shen, K., & Bargmann, C. I. (2008). GFP Reconstitution Across Synaptic Partners (GRASP) defines cell contacts and synapses in living nervous systems. *Neuron, 57,* 353–363.

Field, G. D., & Chichilnisky, E. J. (2007). Information processing in the primate retina: Circuitry and coding. *Annu Rev Neurosci, 30,* 1–30.

Fischbach, K. F. (1979). Simultaneous and successive color contrast expressed in slow phototactic behavior of walking *Drosophila melanogaster*. *J Comp Physiol, 130,* 161–171.

Fischbach, K. F., & Dittrich, A. P. (1989). The optic lobe of *Drosophila melanogaster*. I. A Golgi analysis of wild-type structure. *Cell Tissue Res, 258,* 441–475.

Gao, S., Takemura, S. Y., Ting, C. Y., Huang, S., Lu, Z., Luan, H., Rister, J., Thum, A. S., Yang, M., Hong, S. T., Wang, J. W., Odenwald, W. F., White, B. H., Meinertzhagen, I. A., & Lee, C. H. (2008). The neural substrate of spectral preference in *Drosophila*. *Neuron, 60,* 328–342.

Goldsmith, T. H. (1991). The evolution of visual pigments and colour vision. In P. Gouras (Ed.), *The perception of colour* (pp. 62–89). London: Macmillan.

Gordon, M. D., & Scott, K. (2009). Motor control in a *Drosophila* taste circuit. *Neuron, 61,* 373–384.

Goyret, J., Pfaff, M., Raguso, R. A., & Kelber, A. (2008). Why do *Manduca sexta* feed from white flowers? Innate and learnt colour preferences in a hawkmoth. *Naturwissenschaften, 95,* 569–576.

Hardie, R. C. (1979). Electro-physiological analysis of fly retina .1. Comparative properties of R1–6 and R7 and R8. *J Comp Physiol, 129,* 19–33.

Heisenberg, M., & Buchner, E. (1977). Role of retinula cell-types in visual behavior of *Drosophila melanogaster*. *J Comp Physiol, 117,* 127–162.

Helmstaedter, M., Briggman, K. L., Turaga, S. C., Jain, V., Seung, H. S., & Denk, W. (2013). Connectomic reconstruction of the inner plexiform layer in the mouse retina. *Nature, 500,* 168–174.

Hernández de Salomon, C., & Spatz, H. C. (1983). Colour vision in *Drosophila* melanogaster: Wavelength discrimination. *J Comp Physiol, 150,* 31–37.

Jacobs, G. H. (2009). Evolution of colour vision in mammals. *Phil Trans R Soc B, 364,* 2957–2967.

Joesch, M., Schnell, B., Raghu, S. V., Reiff, D. F., & Borst, A. (2010). ON and OFF pathways in *Drosophil*a motion vision. *Nature, 468,* 300–304.

Karuppudurai, T., Lin, T. Z., Ting, C. Y., Pursley, R., Melnattur, K. V., Diao, F., White, B. H., Macpherson, L. J., Gallio, M., Pohida, T., & Lee, C. H. (2014). A hard-wired glutamatergic circuit pools and relays UV signals to a higher visual center to mediate spectral preference in *Drosophila*. *Neuron, 81,* 603–615.

Kelber, A. (1996). Colour learning in the hawkmoth *Macroglossum stellatarum*. *J Exp Biol, 199,* 1127–1131.

Kelber, A., Vorobyev, M., & Osorio, D. (2003). Animal colour vision—behavioural tests and physiological concepts. *Biol Rev Camb Philos Soc, 78,* 81–118.

Koshitaka, H., Kinoshita, M., Vorobyev, M., & Arikawa, K. (2008). Tetrachromacy in a butterfly that has eight varieties of spectral receptors. *Proc Biol Sci, 275,* 947–954.

Luan, H., Peabody, N. C., Vinson, C. R., & White, B. H. (2006). Refined spatial manipulation of neuronal function by combinatorial restriction of transgene expression. *Neuron, 52,* 425–436.

Meinertzhagen, I. A., & Lee, C. H. (2012). The genetic analysis of functional connectomics in *Drosophila*. *Adv Genet, 80,* 99–151.

Menne, D., & Spatz, H. C. (1977). Colour vision in *Drosophila melanogaster*. *J Comp Physiol, 114,* 301–312.

Menzel, R. (1979). Spectral sensitivity and color vision in invertebrates. In H. Autrum (Ed.), *Comparative physiology and evolution of vision in invertebrates* .(Vol. 7/6/6 A, pp. 503–580). Berlin and Heidelberg: Springer.

Menzel, R., & Greggers, U. (1985). Natural phototaxis and its relationship to colour vision in honeybees. *J Comp Physiol, 157,* 311–321.

Mikeladze-Dvali, T., Wernet, M. F., Pistillo, D., Mazzoni, E. O., Teleman, A. A., Chen, Y. W., Cohen, S., & Desplan, C. (2005). The growth regulators warts/lats and melted interact in a bistable loop to specify opposite fates in *Drosophila* R8 photoreceptors. *Cell, 122,* 775–787.

Morante, J., & Desplan, C. (2008). The color-vision circuit in the medulla of *Drosophila*. *Curr Biol,* 18*,* 553–565.

Nathans, J. (1999). The evolution and physiology of human color vision: Insights from molecular genetic studies of visual pigments. *Neuron, 24,* 299–312.

Neitz, J., & Neitz, M. (2011). The genetics of normal and defective color vision. *Vision Res, 51,* 633–651.

O'Tousa, J. E., Baehr, W., Martin, R. L., Hirsh, J., Pak, W. L., & Applebury, M. L. (1985). The *Drosophila ninaE* gene encodes an opsin. *Cell, 40,* 839–850.

Packer, O. S., Verweij, J., Li, P. H., Schnapf, J. L., & Dacey, D. M. (2010). Blue-yellow opponency in primate S cone photoreceptors. *J Neurosci, 30,* 568–572.

Rister, J., Pauls, D., Schnell, B., Ting, C. Y., Lee, C. H., Sinakevitch, I., Morante, J., Strausfeld, N. J., Ito, K., & Heisenberg, M. (2007). Dissection of the peripheral motion channel in the visual system of *Drosophila melanogaster*. *Neuron, 56,* 155–170.

Salcedo, E., Huber, A., Henrich, S., Chadwell, L. V., Chou, W. H., Paulsen, R., & Britt, S. G. (1999). Blue- and green-absorbing visual pigments of *Drosophila*: Ectopic expression and physiological characterization of the R8 photoreceptor cell-specific Rh5 and Rh6 rhodopsins. *J Neurosci, 19,* 10716–10726.

Sanes, J. R., & Zipursky, S. L. (2010). Design principles of insect and vertebrate visual systems. *Neuron, 66,* 15–36.

Schnaitmann, C., Garbers, C., Wachtler, T., & Tanimoto, H. (2013). Color discrimination with broadband photoreceptors. *Curr Biol, 23,* 2375–2382.

Schnaitmann, C., Vogt, K., Triphan, T., & Tanimoto, H. (2010). Appetitive and aversive visual learning in freely moving *Drosophila*. *Front Behav Neurosci, 4*, 1–10.

Srinivasan, M. V. (2010). Honey bees as a model for vision, perception, and cognition. *Annu Rev Entomol, 55,* 267–284.

Smakman, J. G. J., & Stavenga D. G. (1986). Spctral sensitivity of blowfly photoreceptors: Dependence of waveguide effects and pigment concentration. *Vision Res, 26,* 1019–1025.

Stockman, A., & Brainard, D. (2010). Color vision mechanisms. In M. Bass (Ed.), *OSA handbook of optics* (pp. 11.11–11.104). New York: McGraw Hill.

Sweeney, S. T., Broadie, K., Keane, J., Niemann, H., & O'Kane, C. J. (1995). Targeted expression of tetanus toxin light chain in *Drosophila* specifically eliminates synaptic transmission and causes behavioral defects. *Neuron, 14,* 341–351.

Takemura, S. Y., & Arikawa, K. (2006). Ommatidial type-specific interphotoreceptor connections in the lamina of the swallowtail butterfly, *Papilio xuthus*. *J Comp Neurol, 494,* 663–672.

Takemura, S. Y., Lu, Z., & Meinertzhagen, I. A. (2008). Synaptic circuits of the *Drosophila* optic lobe: The input terminals to the medulla. *J Comp Neurol, 509,* 493–513.

Takemura, S. Y., Bharioke, A., Lu, Z., Nern, A., Vitaladevuni, S., Rivlin, P. K, et al. (2013). A visual motion detection circuit suggested by *Drosophila* connectomics. *Nature, 500,* 175–181.

Tang, S., Wolf, R., Xu, S., & Heisenberg, M. (2004). Visual pattern recognition in *Drosophila* is invariant for retinal position. *Science, 305,* 1020–1022.

Ting, C. Y., Herman, T., Yonekura, S., Gao, S., Wang, J., Serpe, M., O'Connor, M. B., Zipursky, S. L., & Lee, C. H. (2007). Tiling of R7 axons in the *Drosophila* visual system is mediated both by transduction of an activin signal to the nucleus and by mutual repulsion. *Neuron, 56,* 793–806.

Ting, C. Y., McQueen, P. G., Pandya, N., Lin, T. Z., Yang, M., Onteddu, V. R., O'Connor, M. B., McAuliffe, M., & Lee, C. H. (2014). Photoreceptor-derived Activin promotes dendritic termination and restricts the teceptive fields of first-order interneurons in *Drosophila*. *Neuron, 81,* 830–846.

Troje, N. (1993). Spectral categories in the learning behaviour of blowflies. *Z Naturforsch C, 48,* 96–96.

van Hateren, J. H. (1993). Spatial, temporal and spectral pre-processing for colour vision. *Proc Biol Sci, 251,* 61–68.

Wyszecki, G., & Stiles, W. S. (1982). *Color science*. New York: Wiley.

Yamaguchi, S., Desplan, C., & Heisenberg, M. (2010). Contribution of photoreceptor subtypes to spectral wavelength preference in *Drosophila*. *Proc Natl Acad Sci U S A, 107,* 5634–5639.

Yamaguchi, S., Wolf, R., Desplan, C., & Heisenberg, M. (2008). Motion vision is independent of color in *Drosophila*. *Proc Natl Acad Sci U S A, 105,* 4910–4915.